

Rigid-layer modes in chalcogenide crystals

Richard Zallen and Michael Slade

Xerox Rochester Research Center, Rochester, New York 14580

(Received 24 September 1973)

In layer crystals in which the crystal unit cell is two or more layers thick, there appear very-low-frequency zone-center optical phonons in which the layers move very nearly as rigid units. Such rigid-layer modes occur as a consequence of the weakness of the interlayer bonding. Low-temperature Raman scattering experiments on crystalline As_2Se_3 have uncovered the rigid-layer modes in this crystal, as well as many new intralayer modes. The latter have been used to test and extend a scaling relation connecting intralayer frequencies in As_2Se_3 and As_2S_3 . The rigid-layer frequencies have been exploited to derive quantitative information about the interlayer forces. This has been done not only for As_2Se_3 and As_2S_3 , but also for the other cases for which rigid-layer modes have been seen: MoS_2 , GaS, GaSe, and graphite. The results for the interlayer-intralayer force-constant ratio reveal a strong similarity among the chalcogenide layer crystals, despite their structural differences. In the layer chalcogenides, the shear and compressional interlayer force constants are about 60 and 20 times smaller, respectively, than the intralayer covalent-bond force constant. The contrastingly higher anisotropy factors which characterize the greater layerlike character of graphite are, respectively, approximately 10^3 and 10^2 .

I. INTRODUCTION

Layer crystals comprise a class of molecular crystals in which the molecular unit (the individual layer) is macroscopically extended in two dimensions. The molecular symmetry in such two-dimensional-network solids is a diperiodic factor-group symmetry rather than a point-group symmetry as in crystals composed of small molecules.^{1,2} The nature of the weak intermolecular forces which act between the layers and hold such crystals together is poorly understood, although the assumption of van der Waals forces is widely made in the absence of better information.

In layer crystals with more than one layer in the crystal unit cell, there occur very-low-frequency zone-center optical phonons in which the layers move very nearly as rigid units. Termed rigid-layer modes,¹⁻⁵ these vibrations are normally readily accessible to optical experiments such as Raman scattering. Their frequencies provide very direct information about the strength of the interlayer (i. e., intermolecular) forces in these crystals, since for such rigid-layer motions the restoring forces are provided entirely by the layer-layer interactions.

In an extensive Raman and far-infrared investigation¹ of the layer-structure chalcogenides As_2S_3 and As_2Se_3 , it was shown that while the diperiodic symmetry of the individual layer dominates the lattice-vibrational optical properties of these crystals, the weak coupling between layers could be observed as small but discernible symmetry-breaking effects. Thus interlayer-interaction vibrational Davydov splittings, lifting the Raman-infrared degeneracy of internal-mode (i. e., intralayer) frequencies, were observed first in As_2S_3 and As_2Se_3 ¹

and have since been seen in two other layer crystals, MoS_2 ⁶ and GaSe .^{7,8} These splittings indicate that the interlayer force constants in the chalcogenide layer crystals are roughly 100 times smaller than the force constants acting within the covalently bonded layers.

Rigid-layer (RL) vibrations, whose frequencies provide more accurate information about interlayer-intralayer force-constant ratios than do the small interlayer-interaction Davydov splittings (they are of lower order in that ratio) were observed in our room-temperature Raman experiments on As_2S_3 (but not As_2Se_3 , for reasons described below in Sec. II) and have recently been seen in Raman spectra of MoS_2 ,⁴ GaSe ,^{7,8} and GaS .^{8,9} In addition, neutron-scattering data^{3,10} have yielded the RL frequencies in the important case of graphite, the prototype layer crystal.

In the present paper we report the results of low-temperature Raman-scattering experiments on crystalline As_2Se_3 . These data provide the location of low-lying phonon frequencies in this solid including, in particular, the frequencies of the rigid-layer modes. The acquisition of the new information on the low-lying intralayer vibrations allows us to test and extend an empirical scaling relationship connecting vibrational frequencies in As_2Se_3 with those in its isomorphous cousin As_2S_3 . The geometrical complexity of these crystals is a boon for this purpose, since it provides a plentiful supply of internal-mode frequencies and thereby permits a detailed crystal-crystal comparison.

In order to be able to sensibly exploit the data on the very-low-frequency optical phonons, we examine the validity of the notion of rigid-layer modes in the context not only of the two arsenic chalcogenides, but also in that of the other layer-crystal

chalcogenides for which RL data is available, and of graphite. Having done so, the RL eigenfrequencies (in combination with a simple model) are then used to obtain quantitative information on the strength of the interlayer forces. Interlayer-intralayer force-constant ratios are derived which reveal the close similarity which the chalcogenide layer crystals (in spite of their structural differences) display as a group, and which indicate to what extent they are all less layerlike than graphite.

Following the presentation of the As_2Se_3 Raman data in Sec. II, the discussion of the intralayer vibrations and the As_2S_3 - As_2Se_3 scaling relations is given in Sec. III. The analysis of rigid-layer modes is discussed in Sec. IV, and the treatment of the observed RL frequencies to derive interlayer force constants is presented in Sec. V. Our principal findings are summarized in Sec. VI.

II. RAMAN SPECTRUM OF CRYSTALLINE As_2Se_3

In a previous Raman-scattering study of crystalline As_2Se_3 , using 1.16-eV radiation, all Raman lines below 90 cm^{-1} were masked by plasma lines from the exciting (yttrium aluminum garnet) YAG: Nd^{3+} laser used in those experiments.¹ As_2Se_3 is a semiconductor with a room-temperature optical absorption edge of 1.9 eV. In order to be able to use the clean He-Ne laser excitation at 1.96 eV, we have exploited the temperature variation of the As_2Se_3 optical bandgap.¹¹ By cooling the crystal to below 80°K , we could blue-shift the absorption edge sufficiently to render the crystal transparent at 1.96 eV. Measurements were made both with the sample immersed in liquid nitrogen (close to 77°K) and with the sample cemented to the cold finger in the vacuum space of a helium Dewar (about 15°K).

The As_2Se_3 crystals used were vapor-grown plates, about $100\ \mu$ thick, prepared by Griffiths, Keezer, and Vernon of Xerox Research. The crystals were illuminated on a broad face by chopped (400-Hz) radiation from a cw 80-mW He-Ne gas laser, with the Raman emission observed from the sample's edge in a right-angle configuration. A Spex 1400 grating double monochromator, with a photomultiplier and lock-in detection system, was used to analyze the scattered beam. In order to facilitate the intended comparison between the two crystals, low-temperature spectra were also obtained for As_2S_3 (using natural crystals of orpiment¹).

The low-temperature Raman spectrum of crystalline As_2Se_3 is displayed in Fig. 1. Clean spectra were obtained to within 10 cm^{-1} of the laser line. Low-frequency lines have been uncovered at 21.5, 32.5, 53, 57, 77, and 81 cm^{-1} . (The peak positions are determined to an accuracy of $\pm 1\text{ cm}^{-1}$.) New fine structure is also seen in some of the strong

intralayer lines. The dominant Raman band at 251 cm^{-1} reveals triplet structure under high resolution at low temperature, as does the corresponding 357-cm^{-1} band in As_2S_3 shown in Fig. 1 for comparison.¹²

In Fig. 1 we have also included the low-frequency portion of the low-temperature As_2S_3 spectrum, and have indicated the correspondences between the low-lying As_2S_3 and As_2Se_3 lines. As in the case for the high-frequency lines, the correspondences are clear not only by virtue of similarities in positions of lines but also by relative intensities. The As_2S_3 lines at 21.5 and 32.5 cm^{-1} , and to some extent the doublet at 53 - 57 cm^{-1} as well, are those of principal interest here since these involve the rigid-layer vibrations. However, before discussing the interlayer modes and forces, we first accept the opportunity afforded by the detailed information contained in Fig. 1 on the intralayer modes to test the scaling relation suggested earlier¹ for the two arsenic-chalcogenide layer crystals.

III. INTRALAYER VIBRATIONS IN As_2Se_3 AND As_2S_3 - As_2Se_3 SCALING RELATION

The close correlation between the vibrational spectra of As_2Se_3 and As_2S_3 , as exemplified by the corresponding sets of four low-lying lines shown at the right side of Fig. 1 and by the intense high-frequency triplet band shown at the left side, allows the extension of the correspondences to cover essentially all of the observed Raman lines. (In two cases, weak side structure resolved in one crystal was unresolved in the corresponding line of the other.) These empirical spectral correspondences are represented in Fig. 2.

In Fig. 2 we have plotted the frequencies of Raman-active zone-center phonons in As_2Se_3 against the corresponding phonon frequencies in As_2S_3 . Each point in the figure specifies the pair of frequencies, $\bar{\nu}_i(\text{As}_2\text{Se}_3)$ and $\bar{\nu}_i(\text{As}_2\text{S}_3)$, which belong to the same eigenvibration (presumed the same, or very very similar, via the spectral correspondence) in the two closely related crystals. The surprising adherence of these points to a straight line constitutes a considerable quantitative extension of the scaling relation noted earlier¹ on the basis of partial information, and is the subject of this section.

Some information on the structure of these two layer crystals, shown as the insert in Fig. 1, is in order at this point. The rich spectra of Fig. 1, and the detailed crystal-crystal spectral comparison of Fig. 2, are both made possible because of the complexity (20 atoms per crystal unit cell, 10 atoms per layer unit cell) and low-symmetry (C_{2h} crystal symmetry, C_{2v} diperiodic layer symmetry) of the orpiment structure.¹ The complexity is required to provide a large number of zone-center

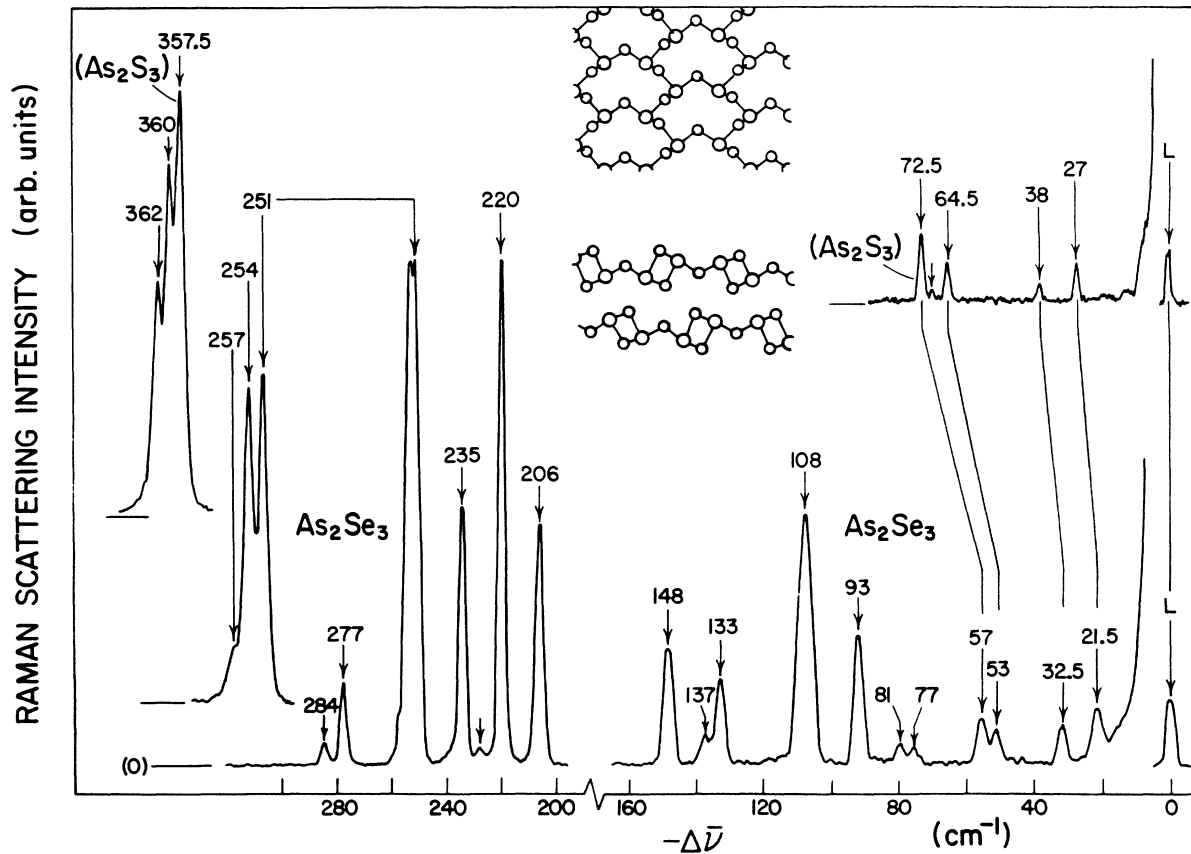


FIG. 1. Raman spectrum of As_2Se_3 at about 15°K. $\Delta\bar{\nu}$ is the frequency shift from the He-Ne laser line at $\bar{\nu}_L = 1.58 \times 10^4 \text{ cm}^{-1}$. Only the Stokes ($\Delta\bar{\nu} < 0$) spectrum is shown since the anti-Stokes intensities are negligible at this temperature. The low-frequency portion of the As_2S_3 low-temperature spectrum is included for comparison, as are high-resolution scans of the dominant triplet bands in both crystals. All linewidths here are instrument limited, as shown by the apparent widths of the attenuated laser lines (L) at the right. The central insert shows the crystal structure, with the upper part providing a broadside view of a single layer and the lower part providing an edgewise view of two adjacent layers.

phonons, and the low symmetry is needed to avoid degeneracies and to permit generous selection rules for Raman activity. For an isolated layer, the 27 intralayer vibrations are all nondegenerate (no symmetry-induced degeneracies) and are all Raman allowed. In the crystal each of the 27 gives rise to a closely spaced doublet, but only one component of each pair is Raman active. (Since both members of each Davydov doublet do not appear together in the scattering spectrum, none of the doublet or triplet fine structure in Fig. 1 can be interpreted in terms of interlayer-interaction Davydov splittings.) In addition, in the crystal there appear the three low-frequency rigid-layer modes, all Raman active. Thus there are 30 possible lines in the first-order Raman spectrum; 18 have been located in Fig. 2 for each crystal.

Because of the anticipated distinction between the behavior of internal (intralayer) and external

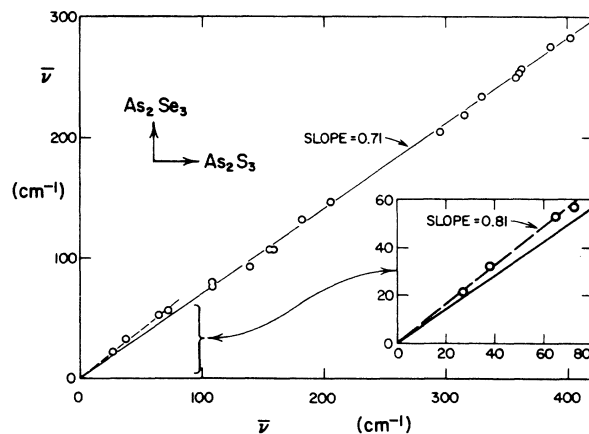


FIG. 2. Frequencies of Raman-active zone-center phonons in As_2Se_3 plotted against the corresponding phonon frequencies in As_2S_3 .

(rigid-layer) modes, the four low-frequency points of Fig. 2 will be treated separately from the 13 high-frequency points. For the 13 intralayer points, the best least-squares fit to a straight line passing through the origin, $\bar{\nu}(\text{As}_2\text{Se}_3) = c_0 \bar{\nu}(\text{As}_2\text{S}_3)$, yields a slope of $c_0 = 0.71 \pm 0.01$ (0.71 is the optimum least-squares slope; 0.01 is the calculated standard deviation of the fitted slope). For the four low-frequency points, the fitted slope is $c_1 = 0.81 \pm 0.05$. The insert in Fig. 2 shows that the low-frequency points do appear to lie systematically, albeit slightly, above the line defined by the high-frequency points. The low-frequency regime, which harbors the information on the RL modes, will be discussed in Sec. V.

The close adherence of the numerous intralayer frequencies to such a simple scaling relation is a remarkable tribute to the isomorphism of these complex crystals, and strong evidence of their very similar vibrational eigenvectors. We can attempt to interpret the 0.71 scaling factor, in terms of the difference in mass between S and Se and the chalcogen substituent effect on the As-X bond-stretching force constant ($X = \text{S}$ or Se), by considering the simplest valence force model and adopting some simplified versions of the layer geometry. The last-mentioned point is necessary since the reduced mass of a mode, which specifies the dependence of the frequency on the atomic masses, depends in detail on the form of the vibrational eigenvector. The intralayer eigenvectors of the actual structure are unknown, so that structural models are needed in order to proceed further. For example, Lucovsky and Martin¹³ have discussed the amorphous forms of the As_2X_3 chalcogenides in terms of a pyramidal AsX_3 molecular subunit. The bond-stretching expressions for the mode frequencies of such an AB_3 molecule, $\omega_0 = \omega_0(k_0, \beta, m_A, m_B)$, have been derived by Herzberg.¹⁴ Here m_A and m_B are the atomic masses, k_0 is the $A-B$ bond-stretching force constant, and β is a geometrical parameter related to the $B-A-B$ bond angle. These expressions factor into the form $\omega_0 = (k_0/\mu_0)^{1/2}$, where the reduced mass μ_0 contains the full dependences of the internal-mode frequency on the geometry and the atomic masses: $\mu_0 = \mu_0(m_A, m_B, \beta)$. The scaling factor $c_0 = \omega_0(\text{As}_2\text{Se}_3)/\omega_0(\text{As}_2\text{S}_3)$ then becomes $c_k c_\mu$, where

$$c_k = [k_0(\text{As}_2\text{Se}_3)/k_0(\text{As}_2\text{S}_3)]^{1/2}$$

and

$$c_\mu = [\mu_0(\text{As}_2\text{Se}_3)/\mu_0(\text{As}_2\text{S}_3)]^{-1/2}.$$

Substituting the values of m_A , m_B , and β appropriate for As_2Se_3 and As_2S_3 into the $\mu_0(m_A, m_B, \beta)$ expressions in the AB_3 molecular model yields c_μ values of 0.74 and 0.77 for the symmetric and

antisymmetric stretching modes, respectively.

As an alternative approach, essayed in order to test the sensitivity of c_μ to the structural model employed, we have also considered a planar version of the A_2B_3 extended layer (a honeycomb lattice with the A atoms at the vertices and the B atoms at the bond centers). This model leads to a value of 0.74 for c_μ .

The three estimates for c_μ cluster around 0.75. Since the observed scaling factor c_0 is 0.71, it follows that the uniform reduction in intralayer frequencies is produced primarily by the influence on the intralayer-mode reduced masses of replacing S by the heavier Se. The results indicate that $c_k^2 = (c_0/c_\mu)^2 \approx 0.9$, implying that the intralayer bonds in As_2Se_3 are about 10% softer than those in As_2S_3 .

IV. ORIGIN OF RIGID-LAYER MODES

Rigid-layer modes are the layer-crystal analogs of the rigid-molecule, or external, vibrational modes occurring in crystals composed of small molecules. The central feature of molecular solids is the coexistence of strong and weak forces and the consequent appearance of distinguishable groups of atoms (molecular units) which mutually interact via the weak forces while being internally bound by the strong. It is possible to distinguish among three general classes of such solids on the basis of the *macroscopic dimensionality* of the molecular unit.² Consider examples of each type selected from among the chalcogenides: As_2Se_3 , trigonal Se, and orthorhombic S. In As_2Se_3 the molecular unit (covalently bonded layer) is macroscopically extended in two dimensions, in trigonal Se the molecular unit (a -Se-Se-Se- helical chain) is macroscopically extended in one dimension, and in rhombic sulfur the molecular unit (a square-antiprism puckered S_8 ring) is not macroscopically extended at all but is finite on an atomic scale. The three distinct types of molecular crystals can be classified as two-dimensional-network, one-dimensional-network, and zero-dimensional-network solids.²

In each type of molecular crystal the rigid-molecule motions are of special interest because of what they reveal about the weak forces. In a zero-dimensional-network crystal composed of nonlinear polyatomic molecules, there are six rigid-molecule degrees of freedom (three translational and three rotational) for each molecule in the unit cell. For a one-dimensional-network (chain-structure) crystal, there are four such external modes (three translational and one rotational) for each chain in the crystal unit cell.² (When we state the number of molecules per unit cell for a one-dimensional- or two-dimensional-network crystal, we specify the number of chains or layers intersected by a single unit cell of the crystal structure.)

For a two-dimensional-network (layer) crystal there are no rotational degrees of freedom (the molecule possesses no cross section of finite extent) and the external (rigid-layer) modes correspond solely to the three translational degrees of freedom of each layer in the unit cell.

Our interest here centers on the long-wavelength optical phonons at or near the center ($q=0$) of the Brillouin zone. For layer crystals with but a single layer per unit cell (e. g., ^{15,16} CdI₂, α -TaS₂) the only $q=0$ rigid-layer modes are the zero-frequency crystal translations, the zone-center acoustic phonons. The simplest layer crystals exhibiting RL optical phonons are those with two layers per unit cell. With two layers per cell, each vibration of the individual layer gives rise to two vibrations in the crystal. These would be degenerate in the absence of any interaction between layers,¹⁷ but the existence of the weak interlayer interaction lifts the degeneracies and produces a set of closely-spaced Davydov doublets.¹ The Davydov partner of each of the three zero-frequency $q=0$ acoustic phonons is a low-frequency RL optical phonon.

Strictly speaking, only the zone-center acoustic modes correspond to purely rigid motions of the layers, since only for these are the eigenvectors determined by symmetry (translational invariance). For the RL optic modes the rigid-layer character of the motion (all intralayer spacings preserved) is a close approximation but is not exact because of the presence (even for such a simple layer crystal as graphite) of intralayer eigenvectors of the same symmetry. Although these may admix with the RL modes, the great disparity in interlayer-intralayer force constants normally keeps this admixture very small. (Two possible exceptions are discussed in Sec. V.) Thus *the appearance of rigid-layer optical modes does not depend on symmetry but is a consequence of the weakness of the interlayer bonding.*

Six layer crystals, five chalcogenides and graphite, for which information is now available on the RL modes,¹⁸ are listed in Table I. The six share the following salient characteristics: (a) the crystal unit cell is two layers thick; (b) the strong intralayer bonding is primarily (the chalcogenides) or entirely (graphite) covalent; (c) the closest interlayer atom-atom contacts are primarily (As₂S₃, As₂Se₃) or entirely (C, MoS₂, GaS, GaSe) between like atoms; (d) the crystal space group contains centers of symmetry which interchange adjacent layers. Highly schematic topological representations of the intralayer-interlayer bonding configurations in these layer structures are shown in Fig. 3.

Characteristic (a) says that these crystals are of the simplest type which satisfy the minimum-complexity condition for the occurrence of optical RL modes. The combination of (a) and (d) ensures

that these RL modes are of even symmetry (A_g and B_g for As₂S₃ and As₂Se₃; B_g and E_{2g} for the others) so that they are infrared-inactive. Thus in layer crystals of this type there are three zone-center rigid-layer optical phonons, they are inversion-invariant, and they are either Raman-active or are optically silent. Two of these are shear vibrations in which adjacent layers slide over each other in oppositely directed motions parallel to the layer planes, while the third is a compressional vibration in which adjacent layers beat against each other in oppositely directed motions along the normal to the layer plane.

V. RIGID-LAYER FREQUENCIES AND INTERLAYER FORCES IN CHALCOGENIDE LAYER CRYSTALS

The objective is to use the experimental information on the RL modes to gauge the strength of the interlayer forces in layer crystals. Since comparisons among a set of related crystals are very valuable, Table I includes reported data on the chalcogenides MoS₂,^{4,6,19} GaS,^{8,9} and GaSe,^{7,8} in addition to our own data for As₂S₃ and As₂Se₃. To make the list complete in terms of current experimental knowledge,¹⁸ and to provide a convenient calibration point for degree of layerlike character, we add what is known^{3,10,20} about graphite—that nonpareil among layer crystals.

Throughout this section, symbols denoting intralayer quantities will carry subscript 0 while symbols denoting interlayer quantities will carry subscript 1. This in the structural parameters given in the second and third columns of Table I, r_0 is the covalent bond length within the layer (nearest-neighbor $M-X$ or $C-C$ distance, where X is S or Se) while r_1 is the closest interlayer $X-X$ or $C-C$ spacing. For the layer chalcogenides the observed r_1 values are in general somewhat smaller than Pauling's van der Waals spacings of 4.0 Å for Se-Se, 3.7 Å for S-S. The quantity r_1/r_0 , the interlayer-intralayer bond-length ratio, is a rough but revealing structural measure of the molecular-ity (layerlike character) of the crystal: the larger is r_1/r_0 , the weaker the expected layer-layer coupling relative to the intralayer covalent bond. This simple structural criterion reveals the similarity among the chalcogenides, with r_1/r_0 values of 1.5–1.6, and the contrastingly much greater layerlike nature of graphite, for which r_1/r_0 is 2.4.

The bonding configurations in the four distinct structures corresponding to the six crystals of Table I have been schematically displayed in Fig. 3. Key similarities among these were discussed in Sec. IV, however the four structures cover a very wide spectrum of complexity and symmetry. Elemental, planar-layer graphite, with only two

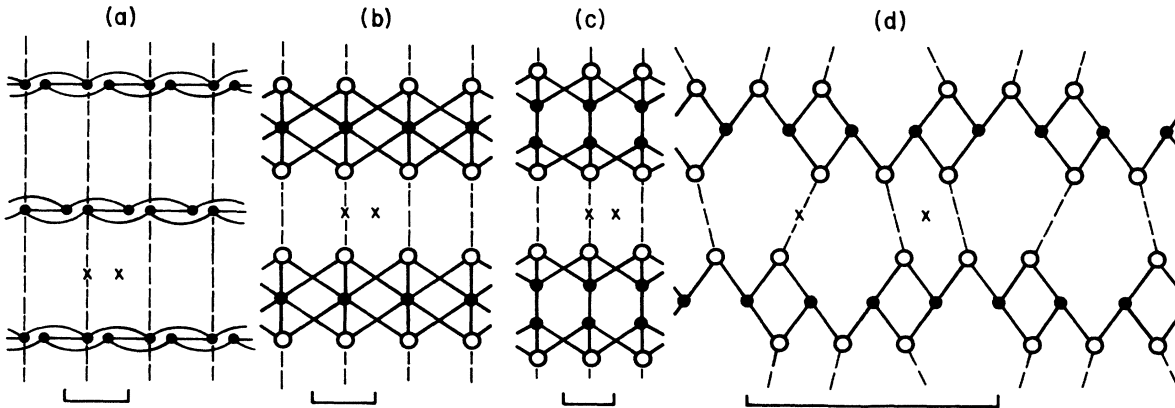


FIG. 3. Highly schematic representations of the four types of layer-crystal structures considered here, viewed with the layers sighted edge on: (a) graphite, (b) MoS_2 , (c) GaS and GaSe, (d) As_2S_3 and As_2Se_3 . The open circles represent chalcogen atoms, the closed circles represent atoms of (a) C, (b) Mo, (c) Ga, or (d) As. The intralayer covalent bonds are represented by the solid lines, with the correct nearest-neighbor coordination shown for each case. The dashed lines represent the density of interlayer "bonds" used in estimating the layer-layer force constants of Table I. Periodicity and symmetry properties are indicated by the horizontal bars (size of the layer unit cell) and the crosses (centers of symmetry in the crystal unit cell).

(four) atoms per layer (crystal) unit cell, has the highest symmetry (D_{6h}) available to a layer crystal. The hexagonal symmetry of the crystal is D_{6h}^4 and of the layer D_{6h}^1 (diperiodic space group $DG80$ in Wood's notation²¹).

In the chalcogenides the atomic positions within the layer are noncoplanar but take on, with some qualifications discussed below, a three-dimensional sandwich structure with the metal atoms inside and the chalcogens outside. There are three atoms per layer unit cell in the MoS_2 structure, four per layer unit cell in the GaS structure, and both are hexagonal crystals (D_{6h}^4 crystal symmetry; D_{3h}^1 , or $DG78$, layer symmetry). The two structures are

intimately related; the coalescence of the pairs of mutually bonded metal atoms in the GaS structure yields the MoS_2 structure. A very large increase in complexity and decrease in symmetry occur when attention shifts to the As_2S_3 structure: 10 atoms per layer unit cell, monoclinic (C_{2h}^5) crystal symmetry, and orthorhombic (C_{2v}^7 , or $DG32$) layer symmetry.

The symmetry difference between the As chalcogenides and the other layer crystals (all hexagonal) of Table I manifests itself in the number of RL eigenfrequencies. In the hexagonal layer crystals the two-dimensional isotropy in the layer plane requires the degeneracy of the two shear RL modes

TABLE I. Rigid-layer phonon frequencies^a and interlayer force constants in chalcogenide layer crystals and graphite.

Crystal	r_1 (Å)	r_1/r_0	$\bar{\nu}_1^{\text{shear}}$ (cm^{-1})	$\bar{\nu}_1^{\text{comp}}$ (cm^{-1})	Rigid-layer mass unit k_1 ----($4\mu_1$)----($4\mu_1$)--	k_1^{shear} ($10^3 \frac{\text{dyn}}{\text{cm}}$)	k_1^{comp} ($10^3 \frac{\text{dyn}}{\text{cm}}$)	$\bar{\nu}_0$ (cm^{-1})	μ_1/μ_0	$\frac{k_1^{\text{shear}}}{k_0}$	$\frac{k_1^{\text{comp}}}{k_0}$
As_2Se_3	3.62	1.51	21.5	~50	r_0 --(Se- $\text{As}_{4/3}$ -Se)----(Se-	1.8	~9	220	1.8	0.021	~0.07
						4.0		251	1.5		
						1.8		315	1.9		
As_2S_3	3.52	1.55	27	~60	---(S- $\text{As}_{4/3}$ -S)----(S-	1.8	~9	357	1.7	0.017	~0.06
						3.5		383 ^d	1.8		
MoS_2	3.5	1.5	34 ^b	56 ^c	---(S-Mo-S)----(S-	2.7	7.4	470	2.6	0.014	0.038
GaS	3.7	1.6	22 ^e		---(S-Ga-Ga-S)----(S-	1.5		294 ^e	2.8	0.016	
GaSe	3.8	1.6	19 ^f		--(Se-Ga-Ga-Se)--	1.6		213 ^f	2.4	0.019	
Graphite	3.35	2.36	45 ^g	128 ^g	\bar{C} ---(\bar{C})----(\bar{C})---	0.7	5.8	1582 ^h	1.5	0.001	0.010

^aThe low-temperature values of Fig. 1 are used for As_2Se_3 and As_2S_3 ; room-temperature values are given for the rest.

^bReference 4.
^cReference 19.

^dReference 6.

^eReferences 8 and 9.

^fReferences 7 and 8.

^gReferences 3 and 10.

^hReference 20.

(which form an E_{2g} doublet), while in the As compounds these are nondegenerate ($A_g + A_g$). In both instances the two shear modes are Raman active, giving rise to one line in the former case and two in the latter. However, for the compressional RL mode, the strict selection rules imposed by the high symmetry require this mode to be optically silent (B_{1g} symmetry) in the hexagonal crystals, while in the As compounds the B_g -symmetry compressional mode is—like the two shear modes—Raman active. Thus while only a single low-frequency RL line shows up in the Raman spectra of C, MoS₂, GaS, and GaSe, we expect to see three such lines in the Raman spectra of As₂S₃ and As₂Se₃.

The large gulf in complexity (unit-cell size) between the arsenic chalcogenides and the other layer crystals also has an important bearing on the nature of the RL modes. In graphite, there is only a single intralayer B_{1g} -symmetry mode which may admix with the compressional RL mode of the same symmetry, and only a single E_{2g} -symmetry intralayer doublet which may admix with the E_{2g} -symmetry shear RL doublet. In MoS₂ there are two such same-symmetry intralayer modes per RL mode, and in GaS and GaSe, there are three. But in As₂S₃ and As₂Se₃, with 54 $q=0$ intralayer vibrations (as discussed in Sec. III), there are 14 B_g -symmetry intralayer modes capable of admixing with the compressional RL mode and 13 A_g -symmetry intralayer modes capable of admixing with the two shear modes! This large number of opportunities greatly increases the chances for occurrence of relatively low-lying intralayer vibrations which can admix with, and thereby reduce the rigid-layer character of, the RL modes. This peril to the RL purity of the three lowest-lying zone-center optical phonons is most threatening in the case of the compressional mode, expected to lie higher in frequency than the shear modes. The interlayer-intralayer admixture for this mode will be seen to be appreciable in both As₂S₃ and As₂Se₃. Such a situation is not encountered in the RL modes of the four simpler layer crystals.

While in what follows the interlayer and intralayer force constants in the various chalcogenides are treated in a uniform manner, there are significant bonding differences which should be noted though their consequences cannot be pursued here. In the hexagonal chalcogenides each chalcogen atom is threefold coordinated within the layer, with one lone pair of nonbonding electrons protruding—along the normal to the layer plane—into the interlayer region. In the arsenic chalcogenides each chalcogen forms two covalent bonds within the layer, with two lone pairs protruding—at various angles—into the interlayer region. Moreover, the view of each layer as a chalcogen-metal-chalcogen

sandwich is only approximately correct in As₂S₃ and As₂Se₃, since the shortest interlayer separations include some As-X spacings mixed in with the dominant X-X spacings.²² [Large liberties have been taken in the schematic structure depicted in Fig. 3(d) relative to the actual one shown in Fig. 1.]

The fourth and fifth columns of Table I contain the inventory of rigid-layer optical-phonon frequencies, denoted as $\bar{\nu}_1^{\text{shear}}$ and $\bar{\nu}_1^{\text{comp}}$, for the five chalcogenides and graphite. For As₂Se₃ and As₂S₃ the low-temperature Raman results of Fig. 1 have been used in order to facilitate the comparison between these two. (The frequency shifts to the room-temperature values are small, but are not yet accurately known for As₂Se₃.) The RL shear-mode frequencies reported for MoS₂,⁴ GaS,^{8,9} and GaSe^{7,8} were determined by Raman scattering, while that for graphite was determined by neutron scattering.^{3,10} The compressional RL mode, optically silent in the hexagonal layer crystals, has been located by neutron spectroscopy for graphite^{3,10} and MoS₂¹⁹; it has not yet been observed in GaS and GaSe.

We assign the pair of low-frequency vibrations, seen at 21.5 and 32.5 cm⁻¹ in As₂Se₃ and at 27 and 38 cm⁻¹ in As₂S₃, to the two nondegenerate shear RL modes of A_g symmetry. The compressional RL mode, of B_g symmetry, is also Raman active in these crystals. There is no indication of a third line in close proximity to the other two, as seen by the narrow width of the two low-frequency lines at low temperature and by the observation that pressure experiments²³ on As₂S₃ reveal no splitting of these lines at pressures (9 kbar) large enough to upshift their frequencies by some 30%. The third-lowest frequency observed in the Raman spectra of both crystals is a member of a doublet, occurring in the vicinity of 50–60 cm⁻¹ in As₂Se₃ and 60–70 cm⁻¹ in As₂S₃. From this observation and from the discussion given earlier on the large number of intralayer modes of equal symmetry to the RL modes, it appears likely that the compressional RL mode has become heavily intermixed with a low-lying (probably bond-bending) intralayer mode.

This interpretation is suggested not only by the sequence of frequencies, but by the As₂S₃-As₂Se₃ frequency relationships shown in Fig. 2. The RL vibrations would not be expected to obey the same scaling relation as that for the intralayer vibrations. For example, the factor $c_\mu = 0.75$ discussed in Sec. III for the intralayer modes takes on the value, for the interlayer modes, of

$$[(2m_{As} + 3m_{Se}) / (2m_{As} + 3m_S)]^{-1/2} = 0.80.$$

The doublet frequencies near 60 cm⁻¹ fall close to the scaling relation observed for the two low-lying RL modes rather than that observed for the intra-

layer modes at higher frequencies, supporting the idea of appreciable RL character in the 60-cm⁻¹ doublet. Approximate values of ≈ 50 and ≈ 60 cm⁻¹, respectively, are entered in Table I for the characteristic compressional-mode rigid-layer vibrational frequencies in As₂Se₃ and As₂S₃.

Interlayer force constants are to be estimated from the RL frequencies $\bar{\nu}_1^{\text{shear}}$ and $\bar{\nu}_1^{\text{comp}}$. Macroscopically, the RL frequencies are determined by quantities averaged over the layer area:

$$\omega = (k_A/\mu_A)^{1/2} = (4k_A/\rho_A)^{1/2},$$

where ρ_A is the layer mass per unit area, μ_A the reduced mass per unit area, and k_A the interlayer spring constant per unit area. In other words, the layers could be treated as continua in discussing these modes. However, because we are interested in effective atom-atom force constants between layers (in order, for example, to compare these with interatomic force constants within the layers), we must explicitly take cognizance of the internal structure of the layer and be specific in the way we relate the interlayer "bonds" to the layer atoms. The way we have chosen to specify the number of interlayer bonds per unit area (in terms of the number of layer atoms per unit area) is indicated by the rigid-layer mass unit listed for each crystal in the center of Table I, which corresponds to the surface density of interlayer bonds represented by the dashed lines in Fig. 3.

For the three types of chalcogenides, the area density of interlayer bonds has been set equal to the surface density of chalcogen atoms (i. e., a single layer-layer "spring" is associated with each pair of chalcogen atoms on facing "surfaces" of adjacent layers). This procedure is a natural one for sandwich-structure layers such as those in MoS₂, GaS, and GaSe, in which the layer surfaces are composed entirely of chalcogen atoms while the metal atoms are buried within the layer interior. It is a bit artificial for As₂S₃ and As₂Se₃, since in these crystals the outside-inside chalcogen-metal distinction is less sharp, though still present; this convention is adopted here also since it is the most reasonable one and since it allows a concrete comparison to the other chalcogenides. For graphite half of the atoms are taken as bonded to both adjacent layers, to be consistent with the interlayer coordination (half of the carbon atoms lie directly above and below atoms on the two adjacent layers, while the other half lie above and below the hexagon centers) and with the idea of interlayer π -orbital overlap in this crystal.

From the above interlayer bond densities and the observed RL frequencies, the atom-atom interlayer force constants may now be determined. Denoting by k_1 the shear or compressional interlayer-bond force constant and by n_A the interlayer bond density

(n_A is the number of interlayer bonds per unit area) specified in each of the above models, the connection with the continuum-layer picture is obtained by setting $k_A = n_A k_1$ and $\rho_A = n_A m_1$, where $m_1 = 4\mu_1$ is the mass (and μ_1 is the corresponding RL-mode reduced mass) of the rigid-layer mass unit composed of the atoms indicated in parentheses in the center column of Table I. For the three simple crystal types of Figs. 3(a)–(c), this RL mass unit coincides with the layer unit cell (two atoms in graphite, three in MoS₂,²⁴ and four in GaSe). However, for the complex orpiment structure of Fig. 3(d), the oversize (ten-atom) layer unit cell contains three such units. The interlayer force constants are now simply determined by $\omega = 2\pi c \bar{\nu}_1 = (k_1/\mu_1)^{1/2}$. The results for k_1^{shear} and k_1^{comp} , for the six layer crystals, are given in columns seven and eight of Table I.

The seven k_1^{shear} values observed for the five chalcogenides lie in the vicinity of $2\text{--}3 \times 10^3$ dyn/cm, ranging from 1.5×10^3 dyn/cm for GaS to 4.0×10^3 dyn/cm for the stiffer shear direction in As₂Se₃. These shear force constants are several times greater than the graphite value of 0.7×10^3 dyn/cm. In contrast to this, the three observed chalcogenide k_1^{comp} values are only slightly larger than that for graphite; all four compressional force constants are about $6\text{--}9 \times 10^3$ dyn/cm. In graphite, the order-of-magnitude difference between k_1^{comp} and k_1^{shear} is understandable as a consequence of the planarity of the layers; to lowest order the shear motion involves only interlayer bond bending while the compressional motion of course invokes interlayer bond stretching. In the chalcogenides the shear motions, as well as the compressional, involve bond stretching also²⁵; in these layer crystals k_1^{comp} is only about three times k_1^{shear} .

It is interesting to compare the results for the three sulfides. The value of k_1^{shear} in MoS₂, and the average of the two k_1^{shear} values in As₂S₃, is 2.7×10^3 dyn/cm, while k_1^{shear} in GaS is significantly smaller at 1.5×10^3 dyn/cm. This difference correlates well with the r_1 values in these crystals. Only in the Ga compound is the sulfur-sulfur interlayer separation as large as the van der Waals diameter; in the other two sulfides r_1 is smaller, symptomatic of stronger interlayer bonding.

Though the k_1 values provide information by themselves, a more illuminating set of quantities to consider (from the viewpoint of quantitatively characterizing the layerlike character of these crystals) are the values of the dimensionless parameter k_1/k_0 , the interlayer-intralayer force-constant ratio. Here k_0 denotes the intralayer bond-stretching force constant of the M - X covalent bond in the chalcogenides or the C-C bond in graphite.

To estimate k_0 we have made use of the intralayer bond-stretching vibrational frequencies shown in column nine of Table I. For each $\bar{\nu}_0$ the simplest bond-stretching valence-force model has been employed to yield the intralayer-mode reduced mass μ_0 appearing in the factored expression $\omega_0 = (k_0/\mu_0)^{1/2}$, as discussed in Sec. III for the intralayer modes in the As compounds. For example, the antisymmetric stretching mode in As_2Se_3 corresponds to the dominant far-infrared reststrahlen band in this crystal¹ and is the Davydov conjugate of the Raman-active mode appearing at $\bar{\nu}_0 = 220 \text{ cm}^{-1}$. In the AB_3 molecular model^{13,14} discussed in Sec. III, the reduced mass μ_0 for this mode is given by $\mu_0^{-1} = 2m_{\text{As}}^{-1} \sin^2(\frac{1}{2}\theta) + m_{\text{Se}}^{-1}$, where θ is the Se-As-Se bond angle. For the Raman-active E_{2g} -symmetry in-plane stretch located at 383 cm^{-1} by Wieting and Verble⁶ in their extensive studies on MoS_2 , the reduced mass may be shown to be given by

$$(3\mu_0 \sin^2 \beta)^{-1} = m_{\text{Mo}}^{-1} + (2m_{\text{S}})^{-1},$$

where β is the angle which the Mo-S bond makes with the normal to the layer plane. For the in-plane stretch in graphite, μ_0 is simply $\frac{1}{3}m_{\text{C}}$. The results for μ_0 are shown in Table I in the form μ_1/μ_0 , since k_1/k_0 is then given directly by $(\mu_1/\mu_0) \times (\bar{\nu}_1/\bar{\nu}_0)^2$.

The deduced values of k_1^{shear}/k_0 and k_1^{comp}/k_0 are presented in the last two columns of Table I. When two intralayer modes were used to yield separate estimates, the average was used for k_0 . Also the k_1^{shear} value used for each of the As compounds, anisotropic in the layer plane, is the average of the two observed shear force constants.

The interlayer-intralayer ratio involving the shear force constants strikingly reveals the strong similarity among the chalcogenide layer crystals, and exposes their sharp difference—as a group—from graphite. For the five chalcogenides, k_1^{shear}/k_0 is bracketed within the narrow range of 0.014–0.021. For graphite this ratio is 0.0012, more than an order of magnitude smaller. Thus while in graphite the interlayer shear forces are about 10^3 times weaker than the covalent forces within the layer, in the layer chalcogenides they are only about 60 times weaker.

Although the information is less complete on k_1^{comp}/k_0 for the chalcogenides (values for three of the five crystals, with two of these approximate), a corresponding—though less-pronounced—distinction is also manifested here. Thus while in graphite the interlayer compressional forces are about 10^2 times weaker than the intralayer forces, in the chalcogenides they are only about 20 times weaker.

Finally, we take note of a small but real difference occurring within each of the two pairs of iso-

morphic crystals included in Table I. For both the arsenic and gallium compounds, the selenide is slightly less layerlike (k_1/k_0 is larger) than the sulfide. For As_2Se_3 and As_2S_3 this has an interesting manifestation in the internal structure of the layer which is possible because the low symmetry of both the crystal and the layer factor groups admits a dimension of flexibility in these layer crystals not present in the others considered. In these crystals there are very slight differences²² between pairs of intralayer bond lengths and bond angles which, though unrelated in the monoclinic crystal symmetry, should be identical in the orthorhombic layer symmetry.¹ These small distortions, which reflect the degree to which the single-layer symmetry is broken by the influence of the surrounding layers, are more perceptible in As_2Se_3 than in As_2S_3 because of the slightly greater importance in the selenide of the interlayer interactions.

VI. SUMMARY

Low-temperature Raman-scattering experiments on crystalline As_2Se_3 have uncovered many low-frequency lines, including those corresponding to the rigid-layer vibrations. The new data on the intralayer modes were used to extend a simple scaling relation connecting As_2Se_3 and As_2S_3 , and to carry out the detailed crystal-crystal comparison shown in Fig. 2. Such a thorough spectral comparison, involving over a dozen pairs of corresponding frequencies, is made possible by the complexity and low symmetry of the orpiment structure. The effect on the intralayer-mode reduced masses of replacing S by the heavier Se comes close to fully accounting for the scaling factor, with the residue indicating that the As-Se bond is slightly softer than the As-S bond.

The principal objective of this paper has been to exploit the rigid-layer vibrational frequencies to derive quantitative information on the strength of the interlayer forces. An analysis of the notion of rigid-layer modes in layer-structure crystals was carried out as a prerequisite for this purpose. The appearance of optical rigid-layer modes is not required by symmetry but is instead a consequence of the weakness of the interlayer bonding. The implications of structure and symmetry (of both the crystal and the isolated layer) for the optical properties of the RL phonons have been treated, not only for complex low-symmetry As_2Se_3 and As_2S_3 , but also for several simpler high-symmetry layer chalcogenides (MoS_2 , GaS, GaSe) for which RL frequencies have been recently determined. Graphite was included to complete the list and to provide an important standard for gauging the layerlike character of the chalcogenides.

Unlike the four hexagonal layer crystals, in each of which there appears but a single Raman-active

RL eigenfrequency, in the arsenic chalcogenides there are three RL Raman frequencies. The two low-frequency Raman lines seen in As_2Se_3 (As_2S_3) at 21.5 and 32.5 (27 and 38) cm^{-1} have been assigned to the two shear RL modes, nondegenerate in these crystals. In both crystals it appears that the compressional RL mode is appreciably admixed with a low-frequency interlayer mode in the neighborhood of 60 cm^{-1} . These two are the only cases, among the 16 RL modes considered, for which the rigid-layer character is appreciably disturbed, a situation abetted by the large size of the layer unit cell (and resultant large number of admixable intralayer modes) in the As_2S_3 structure.

The simple flow diagram for the derivation of interlayer force constants from RL-mode frequencies was outlined in Table I. Besides the experimental frequencies, the other main ingredient is the adoption of a simple model to define the surface density of interlayer atom-atom bonds in terms of the layer structure. In the chalcogenides it is the chalcogen atoms which participate in the interlayer coordination. These sandwich and pseudosandwich structures have been systematically treated in a manner represented in Fig. 3 and in the central column of Table I. The results for the shear interlayer force constants, as well as the less complete results for the compressional interlayer force constants, have been given in the right side of Table I.

In order to have in hand a dimensionless parameter which quantitatively characterizes the layerlike character of these crystals, the above results were combined with intralayer force constants (estimated from internal-mode frequencies) to construct the interlayer-intralayer force-constant ratio shown in the last two columns of Table I. These results, especially those for k_1^{shear}/k_0 , strikingly reveal the strong similarity among the layer chalcogenides (despite the structural differences among them). The degree to which this group of layer crystals is less layerlike than graphite is clearly demonstrated by k_1/k_0 . In the layer chalcogenides k_1^{shear} is about 60 times smaller, and k_1^{comp} about 20 times smaller, than k_0 . The corresponding anisotropy factors in graphite are approximately 10^3 and 10^2 , respectively.

ACKNOWLEDGMENTS

The authors are indebted to J. P. Vernon, C. H. Griffiths, and R. C. Keezer for the vapor-grown As_2Se_3 crystals, and to P. Goldstein for a preprint of his work on the refinement of the structures of As_2S_3 and As_2Se_3 . One of us (R. Z.) wishes to express his gratitude for the hospitality of O. Brafman and E. Cohen of the Technion, Israel Institute of Technology, Haifa, in whose laboratory several early experiments were performed.

- ¹R. Zallen, M. L. Slade, and A. T. Ward, *Phys. Rev. B* **3**, 4257 (1971).
- ²R. Zallen, in *Proceedings of the Enrico Fermi Summer School on Lattice Dynamics and Intermolecular Forces, Varenna, 1972*, edited by S. Califano (Academic, New York, 1973).
- ³G. Dolling and B. N. Brockhouse, *Phys. Rev.* **128**, 1120 (1962).
- ⁴J. L. Verble, T. J. Wieting, and P. R. Reed, *Solid State Commun.* **11**, 941 (1972).
- ⁵While the use of the specific term "rigid-layer modes" was introduced by us in Ref. 1, similar ideas were certainly expressed earlier (for example, in Ref. 3).
- ⁶T. J. Wieting and J. L. Verble, *Phys. Rev. B* **3**, 4286 (1971).
- ⁷T. J. Wieting and J. L. Verble, *Phys. Rev. B* **5**, 1473 (1972).
- ⁸M. Hayek, O. Brafman, and R. M. A. Lieth, *Phys. Rev. B* **8**, 2772 (1973).
- ⁹J. P. van der Ziel, A. E. Meixner, and H. M. Kasper, *Solid State Commun.* **12**, 1213 (1973).
- ¹⁰R. Nicklow, N. Wakabayashi, and H. G. Smith, *Phys. Rev. B* **5**, 4951 (1972).
- ¹¹R. Zallen, R. E. Drews, R. L. Emerald, and M. L. Slade, *Phys. Rev. Lett.* **26**, 1564 (1971).
- ¹²Our low-temperature results for As_2S_3 are in very good agreement with data recently reported by R. J. Kobliska and S. A. Solin [*Phys. Rev. B* **8**, 756 (1973)]. The main differences are that they did not observe the 38- cm^{-1} line at low temperature, and several lines which they labeled as doubtful were confirmed in our experi-

- ments.
- ¹³G. Lucovsky and R. M. Martin, *J. Non-Cryst. Solids* **8**, 185 (1972).
- ¹⁴G. Herzberg, *Infrared and Raman Spectra of Polyatomic Molecules* (Van Nostrand, Princeton, 1964), pp. 155, 163, 176.
- ¹⁵R. W. G. Wyckoff, *Crystal Structures* (Wiley, New York, 1963), Vol. 1.
- ¹⁶J. A. Wilson and A. D. Yoffe, *Adv. Phys.* **18**, 193 (1969).
- ¹⁷J. L. Verble and T. J. Wieting, *Phys. Rev. Lett.* **25**, 362 (1970).
- ¹⁸These six are the only layer crystals known to the authors for which experimental data (via light- or neutron-scattering work) on the rigid-layer vibrations are, thus far, available.
- ¹⁹N. Wakabayashi, H. G. Smith, and R. M. Nicklow, *Bull. Am. Phys. Soc.* **17**, 292 (1972).
- ²⁰L. J. Brillson, E. Burstein, A. A. Maradudin, and T. Stark, in *Physics of Semimetals and Narrow-Gap Semiconductors*, edited by D. L. Carter and R. T. Bate, (Pergamon, Oxford, 1971), p. 187; L. J. Brillson, thesis (University of Pennsylvania, 1972) (unpublished).
- ²¹E. A. Wood, *Bell Syst. Tech. J.* **43**, 541 (1964); *Bell Telephone System Tech. Publ. Monographs* 4680, 1964 (unpublished).
- ²²A detailed analysis of the x-ray-scattering data for As_2Se_3 [A. A. Vaipolin, *Kristallografiya* **10**, 596 (1965)] and As_2S_3 [N. Morimoto, *Mineral J. (Sapporo)* **1**, 160 (1954)] has recently been carried out by P. Goldstein

(unpublished). The values of r_1 and r_0 given in Table I for the arsenic chalcogenides are based on averages of the interlayer and intralayer spacings obtained in Goldstein's refinement of the two crystal structures.

²³R. Zallen, Phys. Rev. B (to be published).

²⁴The MoS₂ value of $k_1^{\text{shear}} = 2.7 \times 10^3$ dyne/cm was obtained earlier in Ref. 4 by using one "formula unit" (i. e., the three atoms of one MoS₂ "molecule") as the appropriate mass unit. This convention is (fortuitously) equivalent to ours in the case of MoS₂, but is not in more complicated cases such as As₂S₃ and As₂Se₃.

²⁵This is evident from the edge-on view of the As₂S₃ structure shown in Fig. 1, but is not evident from the schematic representations of the MoS₂ and GaS structures shown in Fig. 3. In the latter two structures the chalcogen atoms which comprise a layer surface form a triangular lattice, and each atom on the surface of one layer is nested over a triangle of atoms on the facing surface of the adjacent layer. A shear displacement between adjacent layers significantly alters layer-layer interatomic overlaps.